ORBIT CONSTELLATION SAFETY ON THE PRISMA IN-ORBIT FORMATION FLYING TEST BED

Robin Larsson[(1)], Joseph Mueller[(2)], Stephanie Thomas[(2)], Björn Jakobsson[(1)], Per Bodin[(1)]

[(1)]Swedish Space Corporation, P.O. Box 4207, SE-171 04 Solna, Sweden, Email: robin.larsson@ssc.se
[(2)]Princeton Satellite Systems, 33 Witherspoon St. Princeton, NJ 08542, USA, Email: jmueller@psatellite.com

ABSTRACT

PRISMA will demonstrate Guidance, Navigation, and Control strategies for advanced autonomous formation flying. The Swedish Space Corporation (SSC) is the prime contractor for the project which is funded by the Swedish National Space Board (SNSB).
The mission consists of two spacecraft: MAIN and TARGET. The MAIN satellite has full orbit control capability while TARGET is attitude controlled only.
PRISMA will perform a series of GNC related formation flying experiments. SSC is responsible for three main sets of experiments: Autonomous Formation Flying, Proximity Operations and Final Approach/Recede Manoeuvres, and Autonomous Rendezvous.
Many formation flying scenarios, including experiments on PRISMA, require the use of orbits that are not naturally safe. This includes trajectories that, if nominal orbit control were lost, could result in collision or formation evaporation -- secular drift that could eventually cause the loss of relative navigation. This paper will focus on the relative orbit safety concept within PRISMA, presenting the detection and recovery algorithms developed.

1. INTRODUCTION

The PRISMA technology in-orbit test bed implements Guidance, Navigation, and Control (GNC) strategies for advanced formation flying and rendezvous. The Swedish Space Corporation (SSC) is the prime contractor for the project which is funded by the Swedish National Space Board (SNSB). The project is further supported by the German Aerospace Center (DLR), the Technical University of Denmark (DTU), and the French Space Agency (CNES).

The contribution of Princeton Satellite Systems (PSS) to the PRISMA mission is a part of a general cooperative research and development agreement between SSC and PSS that goes back several years. This cooperation aims at developing and expanding the capabilities of the two companies within formation flying and rendezvous and docking technology. E.g. the safe orbit guidance of PRISMA picks up and builds upon PSS' work on quasi passive T-periodic orbit control and collision detection for NASA and the US Air Force, [20,21]. An important purpose and objective for the PRISMA mission is to provide generic solutions valid for many different RVD and FF situations. Including close proximity operations and final approach and recede manoeuvres that do not allow using inherently safe relative orbits. The safety aspects of these situations trigger several interesting problems. Robust solutions for these problems are considered urgent and important.

By the spring of 2008, the project is well into the system integration and test phase. Launch is scheduled for June 2009 with Dnepr. More details on the PRISMA mission in general can be found in [1,2,3].

The objective of PRISMA is to develop and qualify new technology necessary for future space missions. This applies to both hardware qualification as well as several sets of GNC experiments for formation flying.

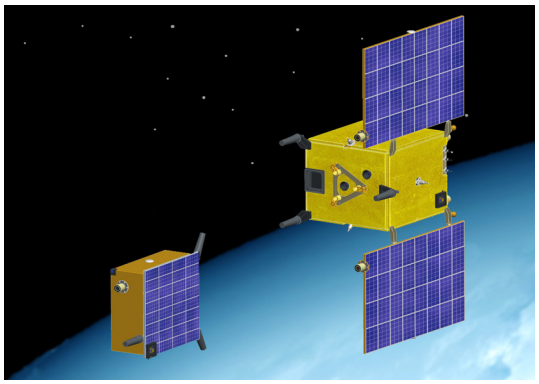

Fig. 1. PRISMA satellites, TARGET (left) and MAIN.

The mission consists of two spacecraft: MAIN and TARGET. The MAIN satellite is 3-axis stabilized and is equipped for full 3D delta-V manoeuvrability independent of its attitude. The TARGET satellite has a simplified, still 3-axis stabilizing, magnetic attitude control system [5] and no orbit manoeuvre capability. An impression of the two spacecraft in orbit is shown in *Fig. 1*.

PRISMA carries a vision based sensor (VBS) provided by DTU [6], a GPS system from DLR [7,8], and an RF-based sensor provided by CNES [9]. MAIN also carries

a Digital Video System (DVS) used to observe and document the formation flying experiments.

The GNC experiment sets consist of closed-loop experiments conducted by SSC [1,10], DLR [11], and CNES [9]. Table 1 summarizes the primary objectives of the PRISMA mission and the corresponding responsible organization.

Table 1. PRISMA primary mission objectives.

GNC Experiment Sets	
PASSIVE FORMATION FLYING	
Autonomous Formation Flying	*SSC*
Autonomous Formation Control	*DLR*
RF-based Formation Flying	*CNES*
FORCED MOTION	
Proximity Operations *Final Approach/Recede Manoeuvres*	*SSC*
Forced RF-based motion	*CNES*
Autonomous Rendezvous	*SSC*
Hardware Related Tests	
HPGP Motor Tests	*ECAPS*
Microthruster Tests	*NanoSpace*
VBS Sensor Tests	*DTU*
RF Sensor Tests	*CNES*

The PRISMA mission also has a set of secondary mission objectives where it will

- Provide a test flight for newly developed system unit and power control unit with battery management electronics (SSC).
- Act as test project for new model based development of on-board software [12] (SSC).
- Demonstrate Autonomous Orbit Keeping of a single spacecraft (DLR).

There are three SSC GNC experiment sets among the primary mission objectives:

- Autonomous Formation Flying [1,13]
- Proximity Operations and Final Approach/ Recede Manoeuvres [1,13]
- Autonomous Rendezvous [1,24]

Ensuring the platform safety is a top priority during all phases of the mission. This paper will describe the relative safe orbit concept including detection and recovery, since it is a new development even though not considered an experiment.

2. PLATFORM AND GNC OVERVIEW

This section will give an overview of the MAIN spacecraft in general and the GNC subsystem in particular. For a more detailed description of MAIN and TARGET, see [1].

2.1. MAIN

The MAIN spacecraft has both attitude and orbit control capability. It is equipped with sun sensors, magnetometers, coarse rate sensors, autonomous star tracker and a set of accelerometers. The actuators are magnetic torque rods, reaction wheels, and hydrazine thrusters. The basic attitude control functionality is based on the SMART-1 attitude control system [14,15].
There are six 1 N nominal hydrazine thrusters arranged in three perpendicular oppositely directed pairs. In addition to these thrusters, there is a fourth oppositely directed pair of HPGP thrusters [4]. This pair is aligned such that it can replace any of the nominal pairs still providing full 3D delta-V capability.
The MAIN spacecraft mode architecture is illustrated with *Fig. 2*.

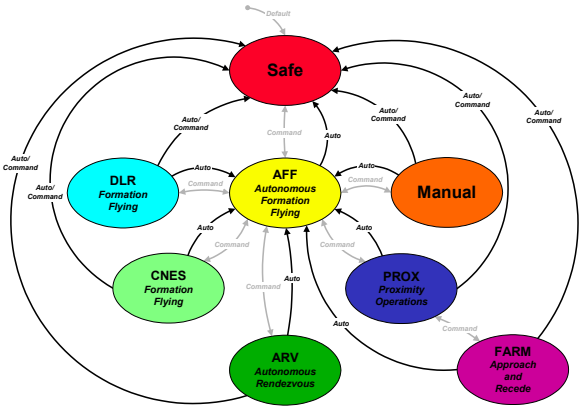

Fig. 2. Mode architecture of the MAIN spacecraft.

There is basically one mode for each group of GNC experiments. The AFF mode is placed as a hub among the operational modes. The reason for this architecture is that this mode consists of very basic functionality including GPS navigation needed also in the safe mode. In addition, the AFF mode implements passive formation flying which makes it particularly suitable for use as a transfer mode between experiments and as a parking mode to be used during performance evaluation. In addition, there is a Safe Mode providing attitude safety as well as safe orbit control. The safe orbit control is described in detail in Section 4.
The safe mode can be entered from every other mode either automatically or through a telecommand. Automatic transitions include requests from the current mode to fall back to safe mode or from anomaly detection, for example when a collision is predicted. Detection of collisions that may occur within a specified time frame is done by a dedicated task which will be described in Section 3. The Collision and Evaporation Detection task is enabled in all GNC modes, but with different settings, to allow safe, monitored operations when MAIN and TARGET are very close but also when distances are large. Safe orbit control is only enabled ones the Safe Mode has been entered.

The safe mode is also automatically entered when starting up the GNC system. This is important to ensure platform safety in case of a processor reset. In the case of a reset, a safe relative orbit can be entered directly using the orbit navigation data which was available before the reset.

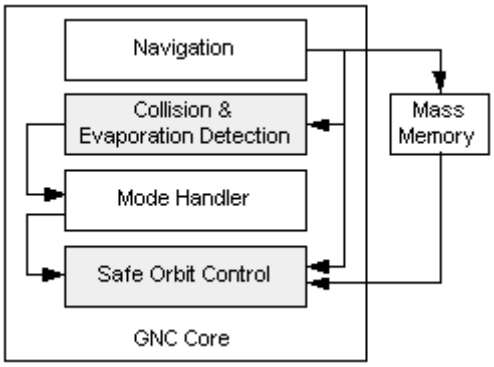

Fig. 3. Signal flow for the orbit safety concept. Go to Safe request to Mode Handler can be manual (TC) or automatic (Collision & Evaporation Detection or request from higher mode guidance functions). Mode Handler enables Safe Orbit Control which will use new or stored Navigation data depending on availability.

Each time there is valid navigation data, a subset of this is written to a certain place in mass memory. This ensures that if the navigation function is invalid. Data from mass memory can be propagated, by the safe orbit control, and used for a limited time to initiate a safe relative orbit.

3. COLLISION MONITORING

Collision detection for PRISMA is a combination of contact computation when they are very close, as is possible during the approach and recede experiment, and predictive collision monitoring for modes when the spacecraft are far enough apart that they may be modelled as spheres.

3.1. Contact Computation

Oriented bounding boxes are used for the contact computation. A single box is used for TARGET, and three boxes for MAIN, including the bus and two solar array boxes.

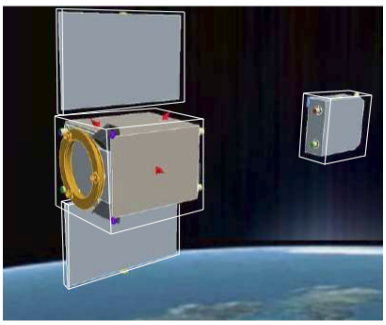

Fig. 4. Bounding boxes for monitoring contact

Upon entering the contact algorithm, a sphere (radius) check is first done to compute the currently estimated minimum distance between the spacecraft. If the sphere check fails, a box check is necessary. If the boxes do not intersect, a minimum distance calculation is performed using the bounding boxes. This minimum distance is the critical monitoring parameter during very close approaches along with the estimated relative velocity. The routine requires one check for each vertex on each box against the other box in a pair, for a total of 16 checks per pair and 48 checks for the whole MAIN spacecraft [22].

3.2. Collision Prediction

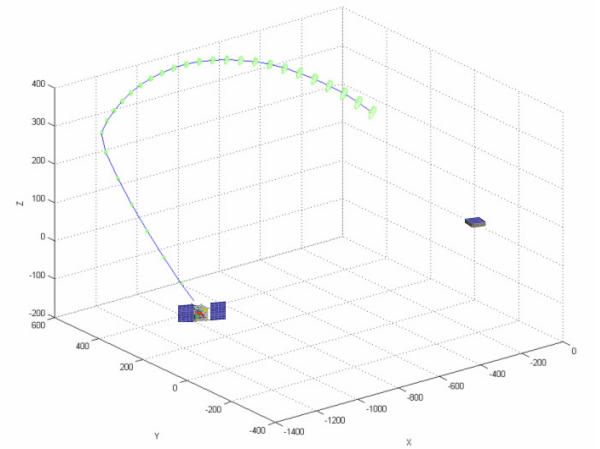

Fig. 5. Illustration of predicted path and uncertainty ellipsoids (green).

The collision monitoring method is based on propagating uncertainty ellipsoids using the relative orbit dynamics [19]. For an ellipsoid S, for example, the 3-sigma relative navigation error (P = 0.997) is propagated using the same discrete matrices as for propagating the nominal trajectory, which corresponds to the ellipsoid centre. The matrix S is the state covariance which is symmetric positive definite and gives the ellipsoid dimensions and orientation. The uncertainty of the dynamics is included in a matrix Q, input covariance, similarly to a Kalman filter. Inputs for MAIN manoeuvres, u_k, can be included:

$$\begin{aligned} x_{k+1} &= A x_k + B u_k \\ S_{k+1} &= A\, S_k\, A' + B\, Q\, B' \end{aligned} \qquad (1)$$

Since the TARGET is passive, we propagate a single relative ellipsoid and compare it to the origin. The ellipsoids are propagated discretely to allow the inclusion of the planned manoeuvres of MAIN. Each delta-V is split over two neighbouring time steps so that the acceleration impulse is centred at the correct time. This allows the probability to be computed for a vector of times.

The probability to collide has conservatively been defined as 1-P(n), where n is the largest sigma relative ellipsoid that does not include any part of the combined radius sphere. Note that n can be a decimal number, as in Fig. 6 where n ≈ 2.5

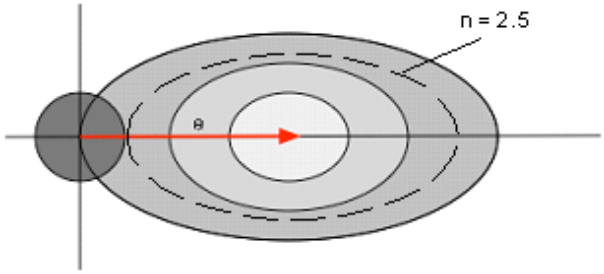

Fig. 6. Conceptual drawing of 1, 2, and 3 sigma relative ellipsoids against the combined radius sphere at the origin

The decision to signal collision detected is based on a GNC mode dependent table. Table 2 shows an example.

Table 2. Estimated time to collision (t_c) versus maximum n to signal collision detected.

t_c[s]	10	30	60	120	240	480	960
n	1	1	0.4	0.4	0.4	0.3	0.3

4. SAFE ORBIT CONTROL

The safe orbit control provides a robust method of achieving safe relative motion between MAIN and TARGET. The prime objective is to ensure the immediate and long-term safety of the spacecraft, in terms of avoiding collision and preventing formation evaporation, with fuel conservation held as a secondary objective. In addition, the method was designed to be deterministic, using only closed-form, non-iterative algorithms. This ensures reliable solutions are obtained with minimal computation time.
The method is summarized as follows. If the estimated relative position between MAIN and TARGET is within an ellipsoidal avoidance region, then a single-burn separation manoeuvre is performed. This is referred to as *separation guidance*. The manoeuvre is guaranteed to monotonically increase the separation distance and exit the avoidance region within a prescribed time. If the sensed relative position is outside the avoidance region, then a manoeuvre is planned to achieve a desired safe relative trajectory. This is referred to as *nominal guidance*. The safe relative trajectory is one that cannot intersect the ellipsoidal avoidance region, even in the presence of uncorrected along-track drift.

The nominal guidance algorithms are designed to maintain a safe trajectory, keeping the two spacecraft sufficiently far apart, and to prevent formation evaporation, keeping the spacecraft sufficiently close for the communication and relative navigation systems to operate. Depending upon the nature of the scenario that leads to Safe Mode, the spacecraft could be performing this safe orbit maintenance for long periods of time, so it is also important to ensure that this aspect of the guidance strategy is fuel efficient.

4.1. Avoidance Region

The avoidance region is a 2x1x1 ellipsoid centred around the TARGET, with semi major axis *d*. Diagram of the avoidance region in the Spacecraft Local Orbit (SLO) reference frame is shown in Fig. 7. The Z axis points in nadir direction, the Y axis is normal to the orbital plane, opposite the angular momentum vector. The X axis completes the right-hand system. To increase the performance, the in-track and cross-track axes are treated as if they where curved. This means that the SLO frame used is not linear but spherical, details can be found in [23]. For practical controlling, there is also a nominal boundary, which is the avoidance region plus a margin. The goal of the safe orbit guidance is to be outside of this boundary.

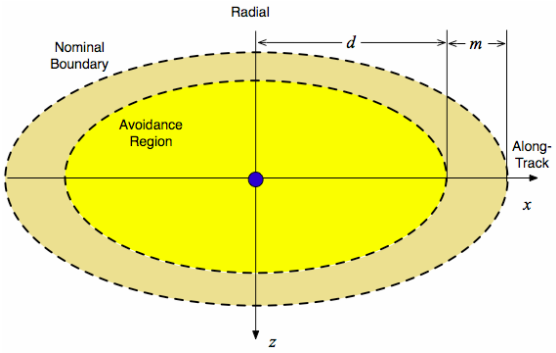

Fig. 7. In-plane projection of the ellipsoidal avoidance region.

4.2. Separation Guidance

In separation guidance, the objectives are to:
1) Exit the avoidance region within a specified time frame.
2) Ensure increasing separation distance while inside the region.
3) Achieve a trajectory that is "uncontrolled safe". The term "uncontrolled safe" refers to a trajectory that never re-enters the avoidance region, even in the event that subsequent control is lost. The period of time by which the region must be exited is a tunable parameter. Smaller times lead to higher delta-vs.

In addition to meeting the above objectives, the algorithm must be computationally simple and deterministic to ensure that a valid, trusted solution is always available without delay. It must also be robust to practical levels of uncertainty in the initial relative

position and velocity estimate used to plan the manoeuvre. An efficient algorithm has been developed that accomplishes all of the objectives with the largest expected levels of navigation uncertainty.

The desired in-plane velocity is first computed with a nominal magnitude V and direction $\hat{u}$, based solely on the position vector. The direction is aligned with the position vector. The magnitude is proportional to the distance from the nominal boundary, and inversely proportional to the separation time. Let r_i and v_i be the in-plane components of the relative position and velocity, and let Δt_s be the separation time. The desired separation velocity v_i^* is initially computed as follows:

$$\hat{u} = \frac{r_i}{\|r_i\|} \tag{2}$$

$$V = \frac{d + m - \sqrt{x^2 + 4z^2}}{\Delta t_s} \tag{3}$$

$$v_i^* = V\hat{u} \tag{4}$$

The delta-v to achieve this is just $v_i^* - v_i$. The direction of this delta-v is immediately checked. If MAIN was already flying away from the TARGET at a higher velocity than v_i^*, then the desired velocity is reset to the original, sufficient velocity.

Nest, the properties of the along-track motion are computed. These result from the new initial state, $[r_i^*, v_i^*]$. The properties include the initial centre of motion x_c, the drift per orbit D, and the amplitude of oscillation A. These parameters are derived from the Clohessy-Wiltshire equations. The equation for $x(t)$ is:

$$\begin{aligned} x(t) = {} & (4v_x / n - 6z)\sin(nt) - 2v_z / n \cos(nt) \\ & - (3v_x - 6zn)t + x + 2v_x / n \end{aligned} \tag{5}$$

The sine and cosine terms give the amplitude, the coefficient for the time gives the drift, and the constant term is the centre of motion. n is the orbital rate of TARGET.

The parameters of interest are calculated as:

$$x_c = x + 2v_x / n \tag{6}$$

$$D = -(2\pi / n) \times (3v_x - 6zn)t$$

$$A = 2\sqrt{(2v_x / n - 3z)^2 + (v_x / n)^2} \tag{7}$$

The objective is now to determine whether the desired initial velocity will re-enter the avoidance region. Upon analysis of the Clohessy-Wiltshire equations, it can be seen that reentry of the avoidance region is possible if any of these two cases holds:

1) The drift rate is too small, so that:

$$|D| < 2d \tag{8}$$

2) The direction of drift is opposite of the initial along-track centre, and the ratio of amplitude to drift is too high:

$$Dx_c < 0, \quad \left|\frac{A}{D}\right| > \frac{1}{2} \tag{9}$$

If either condition holds, then the x-component of velocity is recomputed such that $D = 2ds$, where $s = \pm 1$ is the sign if the drift, selected to match the sign of x_c. The solution for v_x is:

$$v_x = -\frac{n}{3}\left(\frac{fds}{\pi} - 6z\right) \tag{10}$$

where $f \geq 1$ is a tunable safety factor that can be set according to the expected uncertainty in the initial state, to ensure acceptable performance.

A Monte Carlo simulation was conducted with 2000 runs, using random initial conditions inside an avoidance region with d = 60 meters. The sensor noise was modelled at 10 cm standard deviation in relative position, and 10 mm/s in relative velocity (1-sigma). Choosing a safety factor of f = 3 results in 19 cases that re-enter the avoidance region. Increasing f to 4 and then 5 brought the number closer to zero. Doubling to f = 6 resulted in zero re-entries. This indicates that the safety factor either should be defined statically to handle the worst-case noise levels, or it should be made a function of the covariance so that increases with higher noise.

4.3. Safe Ellipse

Once MAIN has exited the avoidance region, it plans manoeuvres to cancel the along-track drift and to enlarge the relative motion in the radial - cross-track plane such that the avoidance region can be encircled. In circular orbits, the relative motion between close-orbiting spacecraft can be expressed geometrically as the superposition of along-track offset, along-track drift, coupled radial and along-track oscillation, and decoupled cross-track oscillation. For relative trajectories that repeat each orbit period, so-called T-periodic trajectories, bounded in-plane oscillations form a 2x1 ellipse, with the elongated axis in-line with the along-track direction. This is evident from the well-known Clohessy-Wiltshire or Hill's equations. Neglecting perturbations for the moment, the period of oscillation in the orbital plane is the same as that in the cross-track direction. It is therefore a simple exercise to construct a relative trajectory that combines radial, along-track and cross-track oscillations so that the motion orbits around the origin. In the presence of along-track drift, the motion appears to corkscrew, circling in the radial / cross-track plane while drifting in

the along-track direction. An example is shown in Fig. 8 for illustration.

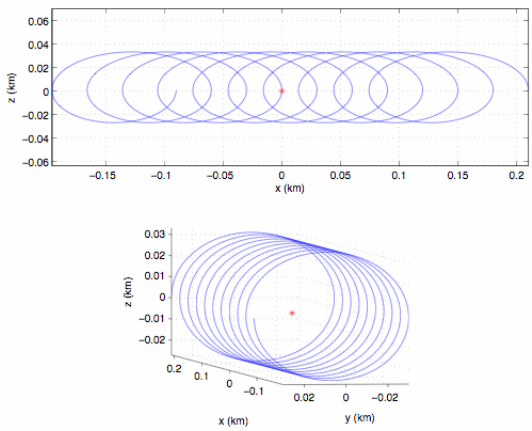

Fig. 8. Illustration of a drifting safe ellipse.

The safe orbit nominal guidance seeks to achieve a safe ellipse that is large enough to encircle the avoidance region.

4.4. Nominal Guidance

The Nominal Guidance algorithm computes a safe relative trajectory for the MAIN spacecraft to follow, and the delta-vs required to achieve it. The trajectory is termed a "safe ellipse". Nominal guidance consists of two basic functions, along-track drift control and radial and cross-track control.

The along-track drift control maintains the drift within a tunable boundary. The drift can be computed using the Clohessy-Wiltshire equations as for separation guidance. Practically this gives unacceptable performance, as even orbits with very small eccentricities will give large oscillations in the estimated drift when the along-track distance is large. A more robust approach is to use the difference between the mean semi-major axis of the TARGET and MAIN orbit.

The radial and cross-track control computes manoeuvres to enlarge the relative orbit to encircle the avoidance region, this is visualized in Fig. 9 and Fig. 10. Normally manoeuvres are only performed to change the size of the semi-minor and semi-major axes of the relative motion in the radial and cross-track plane. This means that no fuel is wasted on shifting the phase of the relative motion, changing θ in Fig. 9 .
It can also be set to gradually decrease the relative orbit in the case of large relative semi-minor or semi-major axes.

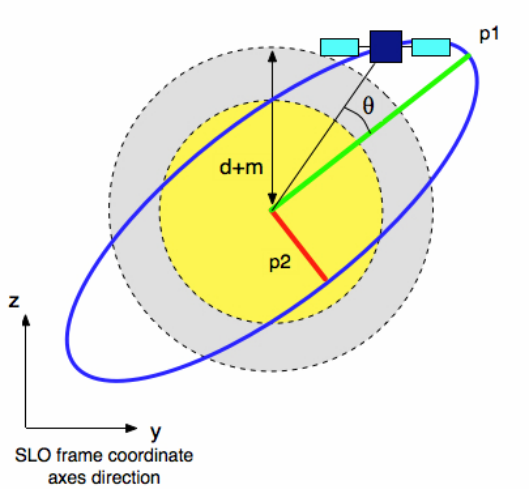

Fig. 9. Unsafe initial relative orbit, intersects the avoidance region.

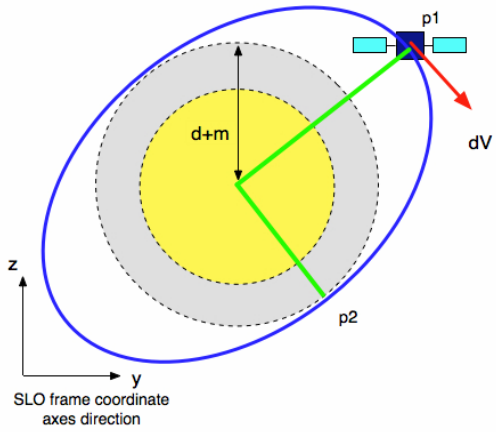

Fig. 10. Corrected safe relative orbit and correction maneuver. Only p2 is extended, p1 is kept at its original location.

The radial and cross-track control assumes a circular orbit, which means that the radial (z) and cross-track (y) component can be modelled as two simple harmonics if disturbances are neglected. Practically these two assumptions holds very well, as the motion in radial and cross-track are rather insensitive to eccentricity and disturbances.

$$y(\theta) = y\cos(\theta) + \frac{\dot{y}}{n}\sin(\theta)$$

$$z(\theta) = 4z - \frac{2\dot{x}}{n} + (\frac{2\dot{x}}{n} - 3z)\cos(\theta) + \frac{\dot{z}}{n}\sin(\theta)$$

The term $4z - \frac{2\dot{x}}{n} = \frac{D}{3\pi}$ is the center of the z movement.
This displacement is caused by the drift in along-track. As the centre of the relative motion is shifted, the

avoidance region in z-direction must also be increased with the same distance.

To simplify calculations, the variable transformation $z(\theta) = z(\theta) - \frac{D}{3\pi}$ is used $(\dot{D} = 0)$. This gives

$$z(\theta) = z\cos(\theta) + \frac{\dot{z}}{n}\sin(\theta) = r_z\cos(\theta - \varphi_z) \quad (11)$$

$$y(\theta) = y\cos(\theta) + \frac{\dot{y}}{n}\sin(\theta) = r_y\cos(\theta - \varphi_y) \quad (12)$$

Introducing two help variables,

$$\Delta\varphi = \varphi_y - \varphi_z \quad \theta' = \theta - \varphi_z ,$$

gives two simple expressions for the Y-Z motion:

$$y(\theta') = r_y\cos(\theta' - \Delta\varphi), \quad z(\theta') = r_z\cos(\theta')$$

The distance to the centre of movement is simply

$$r(\theta') = \sqrt{y(\theta')^2 + z(\theta')^2}$$

Calculating $\frac{dr(\theta')}{d\theta'} = 0$ yields one extreme point given by:

$$\hat{\theta} = \frac{1}{2}\arctan\left(\frac{r_y^2\sin(2\Delta\varphi)}{r_y^2\cos(2\Delta\varphi) + r_z^2}\right) + \varphi_z \quad (13)$$

The closest extreme point (p1) is given by

$\theta_c = \hat{\theta} \pm i\pi/2 \quad i = 1,2\ldots$, such that $0 \le \theta_c < \pi/2$.

Once the closest extreme point is known it is a simple calculation using Eqs. 11-12 to determine whether a maneuver is required or not at $p_1 = \left(y(\theta_c), z(\theta_c)\right)$ to ensure that the length of $p_2 = \left(y(\theta_c + \pi/2), z(\theta_c + \pi/2)\right)$ is larger than the avoidance region. If the distance to P_2 is smaller than d, a maneuver is calculated such that:

$$p_2 = (d+m)\frac{p_2}{\|p_2\|}.$$

The described method is used to extend both the semi-minor and the semi-major axis if required.

There may be cases when a maneuver is required but there is not enough time to wait for the optimal location to apply it. A situation like this can occur for a number of reasons, MAIN is about to enter the avoidance region, navigation solution is about to time out, attitude estimation has been propagated for a long time and is about to be invalid and more. In a situation like this it might not be possible to perform a second maneuver and it is important to ensure long term safety with just one delta-v.

Depending on the situation there are two options:

1. MAIN is far enough away from the along-track axis. This allows the performance of one maneuver which relocates one of the extreme points to the current location. At the same time it ensures that both the semi-minor and semi-major axis is long enough such that the resulting relative orbit encircles the avoidance region. This is done using the same algorithms as in normal situations except that $\theta_c = 0$. This is the favored option.
If the initial position is inside the nominal boundary, the maneuver will effectively ensure that MAIN get no closer to the avoidance region than the current distance, visualized in Fig. 11. If the initial position is outside of the nominal boundary the maneuver will ensure that MAIN stays outside.

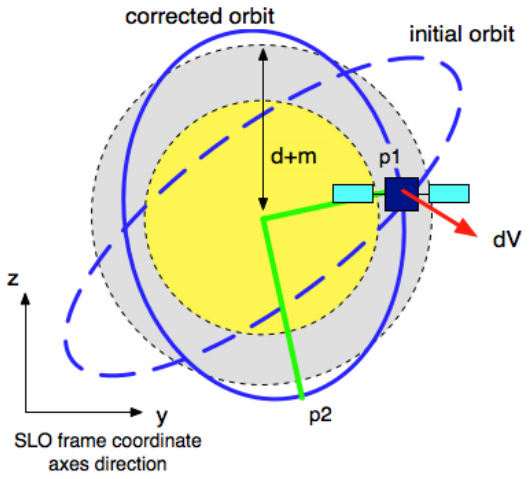

Fig. 11. Single maneuver correction outside avoidance region.

2. MAIN is close to the along-track axis, one delta-v is not enough to put MAIN on a "safe ellipse". The only option is to perform a manoeuvre such that MAIN is placed in an orbit which does not intersect with the avoidance region.

Consider an initial relative position outside of the nominal boundary. Fig. 12 shows the in-plane projection of an example safe ellipse that intersects the current position. There are two degrees of freedom in defining the in-plane portion of the safe ellipse: x_0 and a_E.

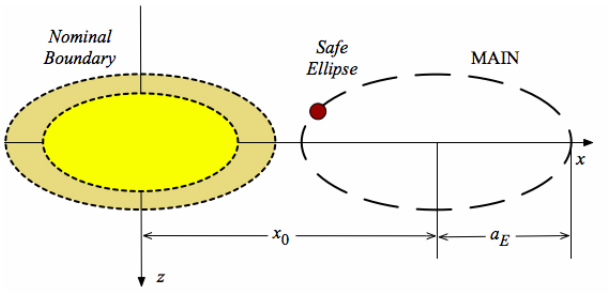

Fig. 12. In-Plane Projection of Safe Ellipse

Because the ellipse must intersect the current in-plane position (*x*, *z*), this effectively eliminates one degree of freedom. Choose x_0 as the control variable. The semi-major axis is then defined as:

$$a_E = \sqrt{(x - x_0)^2 + 4z^2} \qquad (14)$$

The relative velocity required to follow an ellipse from this point is:

$$v_x^* = 2zn$$

$$v_z^* = -\frac{1}{2}(x - x_0)n \qquad (15)$$

n is the orbital rate of TARGET. The out-of-plane velocity has no impact on the in-plane motion, and will therefore remain unchanged. The desired along-track velocity, v_x^*, depends only upon the initial conditions; it is unaffected by the choice of the ellipse. It follows that minimizing the required delta-v is equivalent to minimizing Δv_z, the change in velocity in the *z* direction. As Eq. 15 indicates, this delta-v varies linearly with x_0.

Our objective is to choose x_0 to minimize the required delta-v while respecting the constraints imposed on the relative motion. There are two general constraints on the safe ellipse:

1) The size of the ellipse must be large enough to surround the avoidance region:

$$a_E > d_2 = d + m \qquad (16)$$

The ellipse cannot intersect the nominal boundary:

$$|x_0| - a_E > d_2 \text{ for } |x_0| > d_2 \qquad (17)$$

$$|x_0| + d_2 < a_E \text{ for } |x_0| < d_2 \qquad (18)$$

In Fig. 12, the safe ellipse leads, or is ahead of, the nominal boundary. It clearly satisfies the above constraints. Alternatively, the ellipse could trail the region, or surround it. These three possibilities (lead, trail, surround) correspond to the inequality constraints outlined above.

As a first step the ideal value for the along-track offset is computed. This corresponds to $\Delta v_z = 0$, and the solution is:

$$x_0^* = x + 2v_z / n \qquad (19)$$

The corresponding value for a_E is then computed using Eq. 14 and it is determined whether this ideal value meets all of the constraints. If the ellipse size constraint, Eq. 16, is violated, a new value of x_0^* is computed using Eq. 14 to satisfy the constraint with minimal change in x_0^*. Next, if any of the intersection constraints, Eq. 17-18, are violated, two candidate solutions for x_0^* are computed by treating the inequality constraints as equations. The candidate solutions are:

$$x_0^* = \frac{4z^2 + x^2 - d_2^2}{x + d_2} \qquad (20)$$

and

$$x_0^* = \frac{4z^2 + x^2 - d_2^2}{x - d_2} \qquad (21)$$

These solutions correspond to two feasible ellipses that touch the border of the avoidance region, as illustrated in Fig. 13.

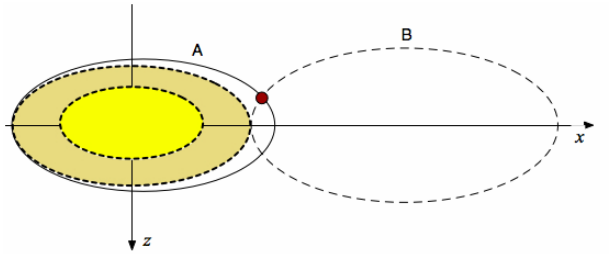

Fig. 13. Example of two possible solutions for the safe ellipse.

The candidate solution that gives the smallest delta-v is selected.

The final step of the safe orbit control includes timing logic, and conditional logic related to the overall fault management plan, which is beyond the scope of this paper.

5. EVAPORATION DETECTION AND CONTROL

Evaporation detection is simply a function of the distance between the two spacecraft. Evaporation is flagged when distances are too large.

Evaporation is controlled by forcing the Safe orbit control to add a drift which is a function of the distance. Nominally the safe orbit control allows a drift which is close to zero.

$$| \text{drift} | < k$$

When the distance d is large, the drift control is biased to allow a drift which is close to an introduced drift.

$$| \text{drift} - \text{introduced\_drift}(d) | < k$$

Where the introduced drift is set such that it will have the opposite sign of the along track distance and growing with the distance up to a certain limit.

6. COMMENTS ON ALGORITHM VALIDITY

The presented algorithms have been developed for use in the PRISMA mission which will have a nearly circular orbit. The primary goal for the development is obviously to provide a robust and reliable safeing of the formation for the PRISMA specific situation, e.g. with respect to the orbit, the allowable separation distances, the navigation metrology, the available processing power, etc. The secondary objective has been to build the development on principles that will apply also in other formation flying situations, with algorithms that are directly applicable or can be expanded and extrapolated to other more demanding formation flying situations, eccentric orbits and other relative navigation metrologies for instance. The ongoing PRISMA developments in the area of optical sighting only navigation is part of that objective and goal.

The overall concept for collision and evaporation detection and control is directly valid also for eccentric orbits with none or small modifications. While the safe orbit control would require additional development, but the basic principles still hold, i.e. separation guidance, nominal guidance with proper phasing between the cross-plane and in-plane motion. The ongoing PRISMA developments within the Autonomous Formation Flying Experiment and the Proximity Operations are parts of that objective and goal. The current Safe Orbit design relies on full orbit GPS for absolute and relative navigation data. Expansion and extrapolation with respect to reduced availability of full orbit GPS data – e.g. HEO orbits, is straight forward and is a matter of orbit propagation and processing power. Safe Orbit for formation flying designs based on non-GPS navigation metrologies, or in orbits beyond the GPS, requires larger modification of the currently implemented navigation filter.

7. SOFTWARE TEST RESULTS

This section presents real-time test results from the relative orbit safety test campaign. An overview of the real-time test environment is given followed by a presentation of test results.

7.1. Test Environment

Testing of the PRISMA GNC subsystem is influenced by the approach taken in [16]. The software is system tested in our in-house developed real-time simulation environment called SatLab. This environment consists of one Engineering Model (EM) computer board for each of the MAIN and TARGET spacecraft. These flight representative boards are connected via a CAN bus to a real-time spacecraft system simulator called SatSim. This simulator simulates all sensors, actuators, space environment, CAN-bus AD/DA conversion and logics for both satellites. As for the on-board software, this simulator is also developed using Matlab/Simulink and generated using automatic code generation. The SatLab simulation environment is controlled with the RAMSES command and control software [17]. RAMSES is used in EGSE as well as in flight and provides script based command and check-out functionality using PLUTO (Procedure Language for Users in Test and Operations) script language [18]. The SatLab environment is illustrated with *Fig. 14*.

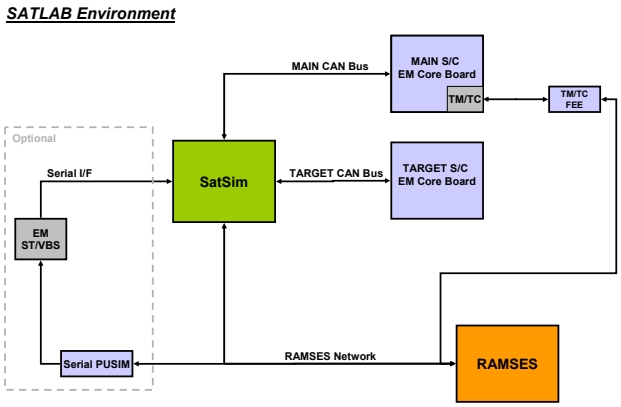

Fig. 14. Schematic of the SatLab test environment.

RAMSES is connected to the MAIN computer board that has integrated TM/TC functionality. It is also connected to the simulator in order to provide start, stop, and reset functionality as well as possibilities to inject errors in sensor and actuator models. Communications with TARGET is done through MAIN using an ISL connection, which is simulated in SatSim.

7.2. Test Results

A subset of the real-time system level test results is presented in this section. In the presented figures, the initial relative position is marked by X, end relative position with a small circle and manoeuvres are indicated by a circle with a line indicating the direction.

The avoidance region with and without margin is shown as two filled ellipsoids. Two examples are presented:

The first example starts with MAIN in a higher GNC mode than Safe. The initial relative orbit is chosen such that a collision will occur about half an orbit later if no manoeuvre is applied. The scenario is visualized in *Fig. 15*-16.
About 1000 seconds from start, a risk of collision is detected which triggers an automatic GNC mode change to Safe, where safe orbit guidance is enabled. Safe orbit guidance has time to perform a normal manoeuvre which is computed to be executed about 500 seconds later, when MAIN will be furthest away from TARGET in the Y-Z plane. The size of the manoeuvre is about 5 cm/s. The resulting orbit has a drift in along-track of about 100 m per orbit. This is within the guidance setting to tolerate up to 150 m per orbit.

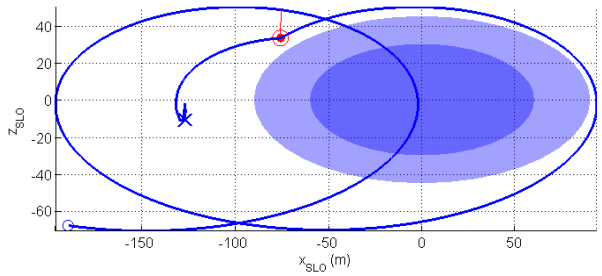

Fig. 15. Along-track and radial view. No correction was made in along-track, that the trajectory encircles the avoidance region in the X-Z plane was not enforced by the safe orbit control.

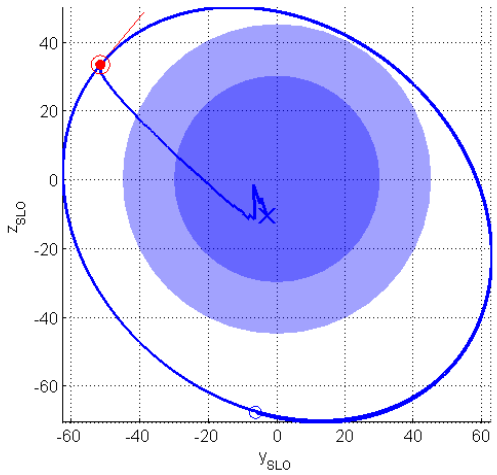

Fig. 16. Cross-track and radial view. The convergence of the GPS navigation filter is clearly visible by the jumps in the start phase.

The second example starts with a fallback to SAFE from a proximity operation. The initial relative state is very close to TARGET. The scenario is visualized in Fig. 17-19.
First the separation guidance requests a manoeuvre, about 7 cm/s, which puts MAIN on a safe drifting relative orbit. Once MAIN is outside the avoidance region nominal guidance calculates a manoeuvre, about 7.5 cm/s, which is applied when MAIN is furthest away from TARGET in the Y-Z plane. This manoeuvre cancels the relative drift and ensures that the minimum distance during one orbit in the Y-Z plane is large enough.

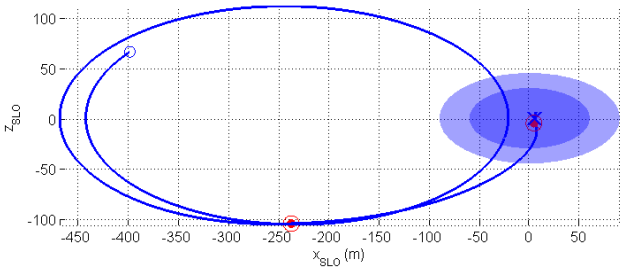

Fig. 17. Along-track and radial view

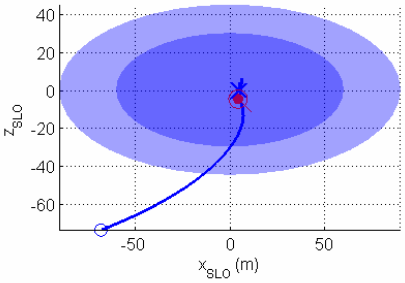

Fig. 18. Close up on the separation phase

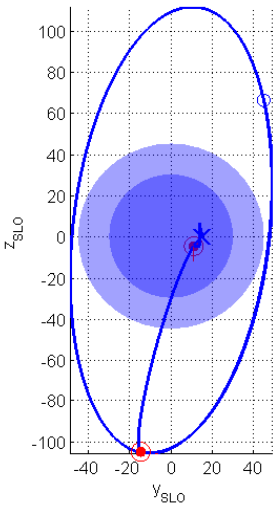

Fig. 19. Cross- track and radial view.

8. CONCLUSIONS

This paper has presented how the platform safety in terms of orbit control is ensured in PRISMA. An overview of the GNC was given followed by a more detailed description of the orbit safety concept. The validity of the algorithms with respect to general orbits was discussed. Finally, the software system test environment was presented including real-time test results from the relative orbit safety test campaign.

9. REFERENCES

1. Persson, S., Jacobsson, B., and Gill, E., *PRISMA Demonstration Mission for Advanced Rendezvous and Formation Flying Technologies and Sensors*, IAF-05-B5.6.B.07, 56th International Astronautical Congress, Fukuoka, Japan, 2005.
2. Persson, S., Bodin, P., Gill, E., Harr, J., and Jørgensen, J., *PRISMA – An Autonomous Formation Flying Mission*, 4S Symposium, Sardinia, Italy, September, 2006.
3. Bodin, P., et al., *Guidance, Navigation, and Control Experiments on the PRISMA In-Orbit Test B*ed, IAC-07-C1.6.01, 58th International Astronautical Congress, Hyderabad, India, 2007.
4. Anflo, K., Persson, S., Bergman, G., Thormälen, P., and Hasanof, T., *Flight Demonstration of an AND-Based Propulsion System on the PRISMA Satellite*, AIAA-2006-5212, 42nd AIAA/AISME/SAE/ASEE Joint Propulsion Conference and Exhibition, Sacramento, California, July 9-12, 2006.
5. Chasset C., Berge, S., Bodin, P., and Jakobsson, B., *3-axis Magnetic Control with Multiple Attitude Profile Capabilities in the PRISMA Mission*, Space Technology, Vol. 26, Issue 3-4, pp 137-154, 2007.
6. Denver, T., Jørgensen, J. L., Michelsen, R., and Jørgensen , P. S., *MicroASC Star Tracker Generic Developments*, 4S Symposium, Sardinia, Italy, September, 2006.
7. Gill E., Montenbruck O., D'Amico S., and Persson S., *Autonomous Satellite Formation Flying for the PRISMA Technology Demonstration Mission*, 16th AAS/AIAA Space Flight Mechanics Conference, Tampa, Florida, Jan. 22-26, 2006.
8. D'Amico, S., Gill, E., and Montenbruck, O., *Relative Orbit Control Design for the PRISMA Formation Flying Mission*, AIAA-2006-6067, AIAA Guidance, Navigation, and Control Conference and Exhibit 2006, Keystone, CO, Aug. 21-24, 2006.
9. Harr, J., Delpech, M., Lestarquit, L., and Seguela, D., *RF Metrology Validation and Formation Flying Demonstration by Small Satellites – The CNES Participation on the PRISMA Mission*, 4S Symposium, Sardinia, Italy, September, 2006.
10. Berge, S., Jakobsson, B., Bodin, P., Edfors, A., and Persson, P., *Rendezvous and Formation Flying Experiments within the PRISMA In-Orbit Testbed*, ESA GNCS 2005, Louthraki, Greece, 2005.
11. Gill, E., D'Amico S., and Montenbruck, O., *Autonomous Formation Flying for the PRISMA Mission*, AIAA Journal of Spacecraft and Rockets, 44/3, 671-681, 2007.
12. Olsson, T. and Edfors, A., *Model-Based Onboard Software Design: The Prisma Case Study*, DAISA 2006 – Data Systems in Aerospace, p. 43.1, Berlin, May 22-25, 2006.
13. Larsson, R., Berge, S., Bodin, P., and Jönsson, U., *Fuel Efficient Relative Orbit Control Strategies for Formation Flying Rendezvous within PRISMA*, AAS 06-025, 29th Annual AAS Guidance and Control Conference, Breckenridge, Colorado, 2006.
14. Bodin P., et al., *The Attitude and Orbit Control System on the SMART-1 Lunar Probe*, 17th International Symposium on Space Flight Dynamics, Vol.1, Keldysh Institute of Applied Mathematics, Moscow, Russia, 2003.
15. Bodin, P. et al., *The SMART-1 Attitude and Orbit Control System: Flight Results from the First Mission Phase*, AIAA-2004-5244, AIAA Guidance, Navigation, and Control Conference and Exhibit 2004 - AIAA Meeting Papers on Disc, Vol. 9, No. 15, AIAA, 2004.
16. Bodin, P. et al., *Development, Test and Flight of the SMART-1 Attitude and Orbit Control System*, AIAA-2005-5991, AIAA Guidance, Navigation, and Control Conference and Exhibit 2005 - AIAA Meeting Papers on Disc, No. 16, AIAA, 2005.
17. Carlsson, A., *A General Control System for Both Sounding Rockets and Satellites*, 18th ESA symposium on European Rockets an Balloon Programmes and Related Research, Visby, June 3-7, 2007.
18. Space engineering: Test and Operations Procedure Language, ECSS-E-70-32A, April 24, 2006.
19. Campbell, M., *Collision Monitoring within Satellite Clusters*, IEEE Transactions on Control Systems Technology, Vol. 13, No. 1, January 2005.
20. Mueller, J., Thomas, S., *Decentralized Formation Flying Control in a Multiple-Team Hierarchy*, Proc. of the 2nd New Trends in Astrodynamics and Applications conference, Princeton, NJ, June 2005. Published in the Annals of the New York Academy of Sciences, Vol. 1065, pp. 112-138.
21. Mueller, J., *A Multiple-Team Organization for Decentralized Guidance and Control of Formation Flying Spacecraft*, AIAA-2004-6249, AIAA Intelligent Systems Conference, Chicago, IL, September 2004.
22. Ericson C., *Real Time Collision Detection*, Morgan Kaufmann Publishers, 2005
23. Lane C., Axelrad P., *Formation Design in Eccentric Orbits Using Linearized Equations of Relative Motion,* AIAA Journal of Guidance, Control and Dynamics, Vol. 29, No. 1, January-February 2006.
24. Nilsson, F., et al. *Autonomous Rendezvous Experiments on the Prisma In-Orbit Formation Flying Test Bed,* Proceedings of the 3rd International Symposium on "Formation Flying, Missions And Technologies", Noordwijk, 23-25 April, 2008.